PHYSICAL REVIEW A **81**, 021401(R) (2010)

Tracing direct and sequential two-photon double ionization of D_2 in femtosecond extreme-ultraviolet laser pulses

Y. H. Jiang,[1] A. Rudenko,[2] E. Plésiat,[3] L. Foucar,[2] M. Kurka,[1] K. U. Kühnel,[1] Th. Ergler,[1] J. F. Pérez-Torres,[3] F. Martín,[3] O. Herrwerth,[4] M. Lezius,[4] M. F. Kling,[4] J. Titze,[5] T. Jahnke,[5] R. Dörner,[5] J. L. Sanz-Vicario,[6] M. Schöffler,[7] J. van Tilborg,[7] A. Belkacem,[7] K. Ueda,[8] T. J. M. Zouros,[9] S. Düsterer,[10] R. Treusch,[10] C. D. Schröter,[1] R. Moshammer,[1] and J. Ullrich[1,2]

[1]*Max-Planck-Institut für Kernphysik, D-69117 Heidelberg, Germany*

[2]*Max-Planck Advanced Study Group at CFEL, D-22607 Hamburg, Germany*

[3]*Departamento de Química C-9, Universidad Autónoma de Madrid, E-28049 Madrid, Spain*

[4]*Max-Planck-Institut für Quantenoptik, D-85748 Garching, Germany*

[5]*Institut für Kernphysik, Universität Frankfurt, D-60486 Frankfurt, Germany*

[6]*Instituto de Física, Universidad de Antioquia, Medellín, Colombia*

[7]*Lawrence Berkeley National Laboratory, Berkeley, California 94720, USA*

[8]*Institute of Multidisciplinary Research for Advanced Materials, Tohoku University, 980-8577 Sendai, Japan*

[9]*Department of Physics, University of Crete, Post Office Box 2208, GR-71003 Heraklion, Crete, Greece*

[10]*DESY, D-22607 Hamburg, Germany*

(Received 12 August 2009; published 23 February 2010)

Two-photon double ionization (TPDI) of D_2 is studied for 38-eV photons at the Free Electron Laser in Hamburg (FLASH). Based on model calculations, instantaneous and sequential absorption pathways are identified as separated peaks in the measured $D^+ + D^+$ fragment kinetic energy release (KER) spectra. The instantaneous process appears at high KER, corresponding to ionization at the molecule's equilibrium distance, in contrast to sequential ionization mainly leading to low-KER contributions. Measured fragment angular distributions are in good agreement with theory.

DOI: 10.1103/PhysRevA.81.021401 PACS number(s): 33.80.−b

Two-photon double ionization (TPDI), that is, the interaction of two photons with two electrons, is among the most fundamental nonlinear processes in atomic [1–8] and molecular [9–12] physics. It is, thus, considered a benchmark reaction to advance nonlinear theories and to explore electron-electron correlations in atoms as well as the coupling between electronic and nuclear motion in molecules beyond the Born-Oppenheimer approximation (BOA). Sparked by experiments that have become feasible at intense high harmonics (see, e.g., [5,6,9]) or ultrabright, free electron laser (FEL) sources such as the Free Electron Laser in Hamburg (FLASH) (see, e.g., [7,8]) and puzzled by the intriguing challenges in predicting the removal of two electrons from He, theoretical interest has just exploded (see. e.g., [1–4] and references therein). Initial attempts to calculate TPDI of molecules [11,12] have been published very recently, which, because of the extreme computational demands, are based on the fixed-nuclei approximation.

As schematically illustrated in Fig. 1 for the D_2 molecule, two different basic TPDI pathways have been discussed in the literature. For "sequential ionization" (SI) the photons (purple arrows in Fig. 1) are assumed to be absorbed via an intermediate *stationary state* of the ion (assumed to be the $1s\sigma_g$ ground state of D_2^+) in two steps, which might be traced in time as indicated by the horizontal arrow. In the direct or "nonsequential ionization" (NSI) channel instead, both photons are absorbed simultaneously through a *virtual intermediate state* as indicated by the left vertical arrows in Fig. 1. Despite tremendous theoretical efforts, questions on the direct ionization of the two He electrons by two photons are not yet settled, not even on the level of total cross sections [4].

On the experimental side as well, the accuracy of total cross section measurements for TPDI has been questioned, since either the statistical significance was weak or, for the FLASH measurements, the intensity of the VUV pulse is not well known due to the uncontrolled time structure of the pulses, emerging from the noise in the self-amplified spontaneous emission (SASE) process. Moreover, in cases where both, SI and NSI are energetically allowed, it was not possible to trace both reactions. For two-photon ionization of H_2/D_2 there exists, to the best of our knowledge, only one experiment [9]. It was found that the production of energetic protons and deuterons proceeds dominantly through two-photon above-threshold ionization but the available intensity was too low (3×10^{12} W/cm^2, 42 eV) for TPDI to be observed.

In this Rapid Communication we demonstrate a method to identify SI and NSI contributions for TPDI of D_2 at 38 eV using a reaction microscope (REMI) [13] to measure the complete fragment-ion momenta. Exploiting the molecule's internal nuclear dynamics (i.e., launching a nuclear wave packet in D_2^+ by the absorption of the first photon; see Fig. 1), we are able to trace SI and NSI contributions via an indirect femtosecond time measurement encoded in the kinetic energy release (KER) spectra for the $D^+ + D^+$ final state. Whereas the direct channel ends at a high energy on the $1/R$ repulsive Coulomb potential curve (where R is the internuclear separation), namely at the equilibrium distance of the neutral molecule, leading to large KERs, sequential ionization, especially from the $1s\sigma_g$ ground state, might result in quite low fragment energies depending on the internuclear separation (i.e., on the time when the second photon was absorbed). Comparing the experimental results to calculations on different levels of approximation we can extract the relative contribution of direct and SI channels, respectively. We further explore the R-dependent ionization probability of D_2^+ in higher vibrational states, study anisotropies in the fragment-ion angular distributions

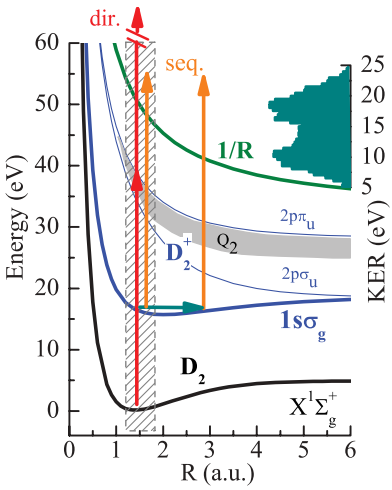

FIG. 1. (Color online) Illustration of the dominant dissociative pathways for single and double ionization of D_2 and experimental KER spectrum for coincident $D^+ + D^+$ fragments created by TPDI via direct and sequential pathways. Depending on the time (horizontal arrow) when the second photon is absorbed after single ionization, the repulsive $1/R$ curve is populated at different R, leading to time-dependent KERs and allowing for the separation of SI and NSI pathways. The gray band indicates doubly excited states Q_2 in Σ and Π symmetries. The Franck-Condon regime is indicated as a vertical shaded band.

(FIADs) for direct and sequential double ionizations, and obtain information on absorption alignment.

In brief, the REMI was installed at the unfocused beam line BL 3 at FLASH [14]. The FEL light first propagates through the main chamber and, then, is focused back onto the target in the REMI by a multilayer focusing mirror mounted behind the main chamber. The mirror has a reflectivity of 40%, being sharply peaked around 38 eV such that higher order harmonic radiation from the FEL is efficiently suppressed to a negligibly low level. Reaching a focus diameter of $\sim$10 μm and having single pulse energies of a few microjoules at a pulse duration of $\sim$30 fs, peak intensities of $I \cong 10^{13}$–10^{14} W/cm^2 were reached at a photon energy of 38 ± 0.5 eV. The focused light beam intersected a well-collimated (0.5-mm diameter) and intrinsically cold supersonic molecular D_2 gas jet propagating transverse to the photon beam direction with densities of up to 10^{10} molecules/cm^3. Ionic fragments were projected by means of an electric field (40 V/cm) onto a time- and position-sensitive microchannel plate detector (with a diameter of 120 mm, position resolution of 0.1 mm, and delay-line read-out). From the measured TOF and position of each individual fragment the initial three-dimensional momentum vectors were reconstructed. The energy resolution in the KER spectra is better than 100 meV for all fragment energies detected.

In order to gain insight into the various one-photon absorption processes, the KER spectrum for noncoincident D^+ fragments, reflecting dissociative channels of D_2^+, is shown in Fig. 2 in comparison with theoretical *ab initio* results using the time-dependent method of [15]. Only fragments emitted perpendicular to the polarization direction ($\theta = 90^\circ \pm 5^\circ$) are considered here. In excellent agreement with the calculations and previous measurements for one-

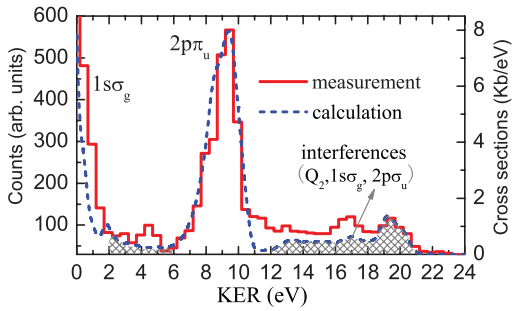

FIG. 2. (Color online) KER spectrum of noncoincident D^+ fragments taken under an emission angle of $90^\circ \pm 5^\circ$ with respect to the light polarization axis (i.e., for final Π symmetry).

photon single ionization [16,17] all relevant fragmentation pathways, such as ground-state dissociation (maximum at $E_{\mathrm{KER}} = 0$), dissociation via the $2p\pi_u$ channel ($E_{\mathrm{KER}} \approx 9$ eV), as well as contributions and interferences involving the decay of doubly excited ($Q2$) states [18], are very well resolved (Fig. 2). In this context it is important to mention that in agreement with both theory and experiment (not shown here), one-photon absorption results with 95% probability in the formation of vibrationally excited D_2^+ molecular ions in the $1s\sigma_g$ ground state. Based on this observation we assume the $1s\sigma_g$ state to be exclusively populated in the first step of sequential TPDI.

We calculate the total SI probability $P_{\mathrm{SI}}^{\mathrm{KER}}$ to a specific KER as a sum over products of one-electron probabilities $P_{\mathrm{SI}}^{\mathrm{KER}} = \sum_v P_1^v \cdot P_2^{v,\mathrm{KER}}$ associated with the two steps (1) D_2 ($v_i = 0$) $\rightarrow D_2^+(v) + e$ and (2) $D_2^+(v) \rightarrow D^+ + D^+ + e$, where, in the BOA,

$$P_1^v \propto \left| \int \left\langle \Psi_i^{D_2}(r, R) \middle| D \middle| \Psi_{\mathrm{el}}^{D_2^+(1s\sigma_g)+e}(r, R) \right\rangle_r \times \chi_{v_i=0}^{D_2}(R)\, \chi_v^{D_2^+(1s\sigma_g)}(R)\, dR \right|^2,$$

$$P_2^{v,\mathrm{KER}} \propto \left| \int \left\langle \Psi_{\mathrm{el}}^{D_2^+(1s\sigma_g)}(r, R) \middle| D \middle| \Psi_{\mathrm{el}'}^{D^+ + D^+ + e}(r, R) \right\rangle_r \times \chi_v^{D_2^+(1s\sigma_g)}(R)\, \chi_{\mathrm{KER}}^{D^+ + D^+}(R)\, dR \right|^2.$$

D is the transition operator for one-photon absorption, $\Psi_i^{D_2}$ is the initial electronic state of D_2, $\Psi_{\mathrm{el}}^{D_2^+(1s\sigma)+e}$ is the electronic continuum state of D_2^+ produced after the absorption of the first photon, $\Psi_{\mathrm{el}}^{D^+ + D^+ + e}$ is the electronic continuum state after the absorption of the second photon; $\chi_{v_i=0}^{D_2}$, $\chi_v^{D_2^+(1s\sigma)}$, and $\chi_{\mathrm{KER}}^{D^+ + D^+}$ are the associated vibrational (dissociative) states; r denotes all electronic coordinates and integration over those is indicated using the usual bracket notation. Integration with respect to the internuclear distance R is explicitly indicated. In this model we are assuming that the two electrons are emitted independently from each other and, consequently, that the time between the two ionization events is infinite (which is reasonable since our pulse duration is larger than a round-trip time of any vibrational wave packet that might be created in the first step). In order to obtain deeper insight into the process we have evaluated these expressions

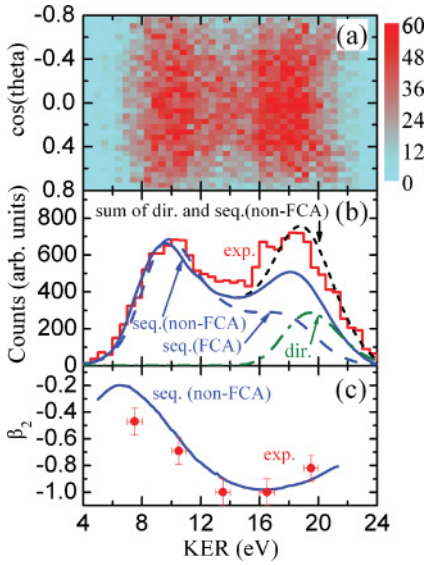

FIG. 3. (Color online) FIAD and KER spectra for coincident $D^+ + D^+$ fragments. (a) Angular distribution of the fragments [$\cos(\theta)$] as a function of the KER; (b) experimental KER spectrum integrated over $|\cos(\theta)| < 0.8$ compared to calculations in the non-FCA and FCA; (c) experimental and theoretical β_2 values as a function of the KER.

by either assuming that the dipole matrix elements do not change with R (what we will later call the Franck-Condon approximation, FCA) or taking explicitly into account their R dependence (the non-FCA).

Similarly, one could also calculate the NSI probability as

$$P_{\mathrm{NSI}}^{\mathrm{KER}} \propto \left| \int \left\langle \Psi_i^{\mathrm{D}_2}(r,R) \middle| D^{(2)} \middle| \Psi_{\mathrm{el}'}^{\mathrm{D}^+ + \mathrm{D}^+ + e}(r,R) \right\rangle_r \times \chi_{v_i=0}^{\mathrm{D}_2}(R) \chi_{\mathrm{KER}}^{\mathrm{D}^+ + \mathrm{D}^+}(R) dR \right|^2,$$

where $D^{(2)}$ is the transition operator for two-photon absorption. Since evaluation of the R dependence of the integral involving the latter operator is prohibitively expensive [12], this probability has been exclusively evaluated within the FCA. Since the calculations do not provide the absolute values of the SI and NSI probabilities, the total probability has been obtained by fitting $aP_{\mathrm{SI}}^{\mathrm{KER}} + bP_{\mathrm{NSI}}^{\mathrm{KER}}$ (where the ratio a/b represents one effective free parameter independent of the KER) to the experimental KER spectra in Fig. 3(b). In doing so we are assuming that the SI and NSI processes do not interfere.

In Fig. 3(a), KER spectra for coincident $D^+ + D^+$ fragments are presented as a function of $\cos(\theta)$, that is, the fragment's emission angle relative to the light polarization axis. The angular integrated KER spectrum together with calculations is plotted in Fig. 3(b). Since some uncertainties due to the dead time of the detector system cannot be excluded at small angles, the integration for the data in Fig. 3(b) extends from $\cos(\theta) = -0.8$ to 0.8. Two clear peaks are visible in the experimental data, one at high KERs between about 16 and 24 eV and a low-energy part extending from ~5 to ~15 eV. As illustrated in Fig. 1, this KER range corresponds to internuclear distances R between ~1.3 a.u., the minimum value within the FC regime, and $R \sim 6$ a.u., which can only be reached via ground-state dissociation of the $1s\sigma_g$ states. As discussed before, we neglect effects <5% that might be due to excitation into the Q_2 band as well as to the $2p\pi_u$ and the $2p\sigma_u$ states. Also plotted in Fig. 3(b) are the results of our model calculations for the non-FC approximation (i.e., by taking realistic R-dependent ionization probabilities into account as well as for the FCA, assuming constant ionization cross sections as a function of R). It can be seen that neither the SI nor the NSI, when considered separately, can reproduce the observed peaks and their relative heights. For the intensities used in the experiment, the correct relative heights can only be obtained if both processes contribute in the high-energy region of the KER spectrum, irrespective of whether they interfere or not. In both the non-FC and FC approximations, the sequential ionization contributes strongly to the low-energy part, displaying a clear peak that largely coincides with the experimental one. Some differences between the two calculations are visible at higher KERs, where the flux obtained within the non-FCA is slightly larger and located at somewhat higher energies than for the FCA. On the basis of the calculations and by inspecting the contributions of different vibrational levels to the spectra (not shown here) an interpretation of our observations is straightforward. We find that the largest contribution to SI originates from the $v = 2$ state followed by those with $v = 1$ and $v = 3$, just reflecting the initial distribution after the absorption of the first photon. The slightly different KER position of the low-energy maximum in the two calculations indicates small differences in the population of vibrational states due to the R-dependent ionization probability in the non-FCA.

Thus, the calculations lead to a straightforward interpretation of the low-energy peak: A set of vibrational levels are excited on the $1s\sigma_g$ potential curve of the D_2^+ molecule after absorption of the first photon. Sequentially, if infinite time in the calculations is assumed, a second photon is absorbed, projecting the corresponding R distribution onto the repulsive $1/R$ potential curve such that the two maxima simply represent the inner and outer turning points of the corresponding vibrational states where the time-averaged density distribution of the states is largest. Since ionization at small R is less likely (because the FC overlap between intermediate and final vibrational states is smaller near the inner classical turning point), the maximum at the high-energy part of the KER spectrum is slightly lower. As the length of the FEL pulse is estimated to be about 30 fs and a wave packet launched in the FC regime would travel to the outer turning point within about 10–12 fs, the time-independent approach, under the assumption that all R on the $1s\sigma_g$ surface are equally populated, seems to be well justified.

It is very obvious, however, that sequential ionization alone cannot explain the experimental high-energy peak in the KER spectrum. To explain this contribution at $E_{\mathrm{KER}} = 18.5$ eV, direct TPDI, where the nuclear wave packet has not moved significantly, is needed in both model calculations [dash-dotted line in Fig. 3(b)]. This provides clear evidence that we do observe experimentally both the direct and the sequential TPDI channels simultaneously and can distinguish between both pathways through an indirect time measurement exploiting the femtosecond nuclear motion. In particular, fragments with low KERs can only be created via the sequential absorption of two

photons projecting the $D_2{}^+$ vibrational states created by the first photon onto the repulsive $1/R$ curve at large internuclear distances.

Several aspects should be kept in mind when comparing the results of the model with experiment: (i) The present calculations add the contributions of both channels incoherently, thus possible interference between both channels is neglected. Similar interference effects were recently predicted to occur in three EUV-photon absorption processes [19]. (ii) The experimental pulse duration is limited to about two round trips of the vibrational wave packet that is launched by the absorption of the first photon such that time-dependent effects, not yet implemented into the calculations, might occur. (iii) We cannot exclude additional experimental effects due to the essentially unknown pulse structure of the FEL, which, depending on the specific settings of the FEL, could change even during a single experimental campaign. Measuring the KER distributions in two different beam times we always find two peaks, but with different relative weights, most likely due to the different actual pulse durations and peak intensities achieved.

Finally, we also inspect the fragment-ion angular distributions. These can be characterized by a multipole expansion in terms of Legendre polynomials, $\frac{d\sigma}{d\Omega} = \frac{\sigma_0}{4\pi}[1+\sum_{i=1,\ldots,n}\beta_{2i}P_{2i}(\cos\theta)]$, where n is the number of absorbed photons and β_{2i} are the asymmetry parameters. FIADs for the coincident $D^+ + D^+$ fragments have been extracted at selected KERs by integrating events within ± 1.5 eV around the respective central value. The corresponding experimental $\beta_2$values from fits together with calculations are presented in Fig. 3(c). The latter have been obtained within the sequential model by assuming a random orientation of the $D_2{}^+(v)$ produced after the first ionization step, that is, $\beta_2 = \sum_v P_1^v \beta_2(v)/\sum_v P_1^v$, where $\beta_2(v)$ is the asymmetry parameter of $D_2{}^+$ in the vibrational states v. Good agreement between theory and experiment is found. Surprisingly, the agreement is also good at high KER where direct ionization, not taken into account in the present calculations, significantly contributes, thus indicating a possible isotropic FIAD for this process. The fragments in between the two peaks display a slightly more pronounced anisotropic angular distribution, $\beta_2 = -1.0$, hinting on an increased contribution of Π symmetry. Finally, within the experimental uncertainties, we do not observe obvious quadrupole contributions (β_4) to the FIADs induced by two-photon absorption.

In summary, two-photon double ionization of D_2 at 38-eV photon energy has been explored by inspecting fragment-ion angular distributions and kinetic energy releases in the $D^+ + D^+$ final channel. We demonstrate that the KER spectra encode the time in between the absorption of the two photons through the internal molecular dynamics, enabling us to distinguish between sequential and direct absorption pathways and thus quantifying their relative contribution. Finally, the FIADs are inspected and show distinct differences for the SI and NSI, being in reasonable agreement with the theoretical prediction for sequential ionization.

The authors are greatly indebted to the scientific and technical team at FLASH, in particular, the machine operators and run coordinators, in striving for optimal beam-time conditions. Computations were carried out at Mare Nostrum BSC and CCC-UAM. We would like to thank E. Louis and F. Bijkerk from the FOM Institute of Plasma Physics in Rijnhuizen along with J. Verhoeven, P. Johnsson, and M. Vrakking from AMOLF for providing the multilayer mirror. Support from the Max-Planck Advanced Study Group at CFEL is gratefully acknowledged. Y.H.J. is grateful for support from DFG Project No. JI 110/2-1, E.P., J.F.P.-T., and F.M. from MICINN Project No. FIS2007-60064, J.L.S.-V. from COLCIENCIAS, J.T., T.J., and R.D. from Koselleck program of the DFG, and O.H., M.L., and M.F.K. from the DFG via the Emmy-Noether program and the Cluster of Excellence: Munich Center for Advanced Photonics. The European COST Action "CUSPFEL" (CM0702) is also acknowledged.

[1] D. A. Horner, T. N. Rescigno, and C. W. McCurdy, Phys. Rev. A **77**, 030703(R) (2008).
[2] X. Guan, K. Bartschat, and B. I. Schneider, Phys. Rev. A **77**, 043421 (2008).
[3] J. Feist *et al.*, Phys. Rev. A **77**, 043420 (2008).
[4] E. Foumouo *et al.*, J. Phys. B **41**, 051001 (2008).
[5] Y. Nabekawa, H. Hasegawa, E. J. Takahashi, and K. Midorikawa, Phys. Rev. Lett. **94**, 043001 (2005).
[6] P. Antoine *et al.*, Phys. Rev. A **78**, 023415 (2008).
[7] A. A. Sorokin, M. Wellhofer, S. V. Bobashev, K. Tiedtke, and M. Richter, Phys. Rev. A **75**, 051402(R) (2007).
[8] A. Rudenko *et al.*, Phys. Rev. Lett. **101**, 073003 (2008).
[9] K. Hoshina *et al.*, J. Phys. B **39**, 813 (2006).
[10] T. Sato *et al.*, Appl. Phys. Lett. **92**, 154103 (2008).
[11] J. Colgan *et al.*, J. Phys. B **41**, 121002 (2008).
[12] F. Morales *et al.*, J. Phys. B **42**, 134013 (2009).
[13] J. Ullrich *et al.*, Rep. Prog. Phys. **66**, 1463 (2003).
[14] K. Tiedtke *et al.*, New J. Phys. **11**, 023029 (2009).
[15] J. L. Sanz-Vicario, H. Bachau, and F. Martín, Phys. Rev. A **73**, 033410 (2006).
[16] K. Ito, R. I. Hall, and M. Ukai, J. Chem. Phys. **104**, 8449 (1996).
[17] T. Havermeier, diploma thesis, Universität Frankfurt, 2006, http://www.atom.uni-frankfurt.de/web/publications/files/Tilo_Havermeier_2006.pdf.
[18] F. Martin *et al.*, Science **315**, 629 (2007).
[19] M. Førre, S. Barmaki, and H. Bachau, Phys. Rev. Lett. **102**, 123001 (2009).